NOT FOR PUBLICATION

Attachment D-4-137

D710

HIGHWAY RESEARCH REPORT

PERFORMANCE OF A REINFORCED EARTH FILL

Presented at the 53rd Annual Meeting
of the Highway Research Board
January, 1974

74-04

STATE OF CALIFORNIA

BUSINESS AND TRANSPORTATION AGENCY

DEPARTMENT OF TRANSPORTATION

DIVISION OF HIGHWAYS

TRANSPORTATION LABORATORY

RESEARCH REPORT

CA-DOT-TL-2115-1-74-04

Prepared in Cooperation with the U.S. Department of Transportation, Federal Highway Administration

ClibPDF - www.fastio.com

ClibPDF - www.fastio.com

TECHNICAL REPORT STANDARD TITLE PAGE

1. REPORT NO.	2. GOVERNMENT ACCESSION NO.	3. RECIPIENT'S CATALOG NO.
4. TITLE AND SUBTITLE Performance of A Reinforced Earth Fill		5. REPORT DATE January, 1974 6. PERFORMING ORGANIZATION CODE 19202-632115
7. AUTHOR(S) Chang, Jerry C., Forsyth, Raymond A., and Beaton, John L.		8. PERFORMING ORGANIZATION REPORT NO. CA-DOT-TL-2115-1-74-04
9. PERFORMING ORGANIZATION NAME AND ADDRESS Transportation Laboratory 5900 Folsom Blvd. Sacramento, CA 95819		10. WORK UNIT NO. 11. CONTRACT OR GRANT NO.
12. SPONSORING AGENCY NAME AND ADDRESS California Department of Transportation Division of Highways Sacramento, CA 95807		13. TYPE OF REPORT & PERIOD COVERED 14. SPONSORING AGENCY CODE

15. SUPPLEMENTARY NOTES

16. ABSTRACT

The data resulting from an extensive instrumentation of the reinforced earth embankment constructed on Route 39, Los Angeles County, California, in 1972 is summarized. A comparison between field behavior predicted by equations developed to evaluate the design and that indicated by instrumentation is also presented. Field measurements evaluated include strain of reinforcing strips, soil pressure, lateral movement, settlement, strap slippage and skin plate deformation.

The instrumentation data reveals reasonably close agreement between design assumptions and field behavior. Based upon the results, recommendations are presented for the design of future reinforced earth installations.

17. KEY WORDS	18. DISTRIBUTION STATEMENT
Reinforced earth, stress, deformation, pulling test, slippage, skin plate, skin friction angle, instrumentation, field performance.	Unlimited

19. SECURITY CLASSIF. (OF THIS REPORT)	20. SECURITY CLASSIF. (OF THIS PAGE)	21. NO. OF PAGES	22. PRICE
Unclassified	Unclassified		

HMRT – 1242 (ORIG. 9/72)

ClibPDF - www.fastio.com

ClibPDF - www.fastio.com

Jerry C. Chang
Raymond A. Forsyth
John L. Beaton

Reference: Chang, Jerry C., Forsyth, Raymond A., and Beaton, John L., "Performance of a Reinforced Earth Fill," State of California, Department of Transporation Laboratory, Federal HPR Project No. D-4-93, October 7, 1970.

ClibPDF - www.fastio.com

ClibPDF - www.fastio.com

State of California
Department of Transportation
Transportation Laboratory

PERFORMANCE OF A REINFORCED EARTH FILL

By

Jerry C. Chang
Raymond A. Forsyth
John L. Beaton

Presented at the 53rd Annual Meeting
of the Highway Research Board
January 1974

ClibPDF - www.fastio.com

ClibPDF - www.fastio.com

PERFORMANCE OF A REINFORCED EARTH FILL

By

Jerry C. Chang[1], Raymond A. Forsyth[2], John L. Beaton[3]

INTRODUCTION

Reinforced earth is a soil mass composed of fill strengthened by metal or plastic reinforcements and enclosed at the front face by skin elements. Since Roman times, builders have been aware of the beneficiating effects of the inclusion of reinforcing elements in earthwork. One example of this is the use of brush by the Dutch in dike construction. The use of earthwork reinforcement based upon a rational design procedure was reported in 1969 by Henri Vidal (1). In October, 1972,

---

[1]Project Engineer, Foundation Section, Transportation Laboratory, Division of Highways, California Department of Transportation, Sacramento, California.

[2]Chief, Foundation Section, Transportation Laboratory, Division of Highways, California Department of Transportation, Sacramento, California.

[3]Chief, Transportation Laboratory, Division of Highways, California Department of Transportation, Sacramento, California.

ClibPDF - www.fastio.com

the first application of reinforced earth to highway construction in the United States was carried out by the California Department of Transportation to reopen a section of Highway 39 in the San Gabriel Mountains, Los Angeles County. This section of Highway 39 had been closed by a surficial debris slide during a heavy spring storm in 1969.

A description of the slide and the rationale for the selection of reinforced earth for its correction were reported by Chang, et al (2) in 1972. That paper also presented the results of the soil investigation and stability analysis in addition to equations developed for analyzing the stresses in the reinforcing strips. Using those equations the size, length, and spacings of the reinforcement suggested by the reinforced earth company, Terre Armee, were evaluated.

In this paper, equations for analyzing the stresses in the skin plates, and the comparisons between the field instrumentation data and the analytical results for both of the reinforcing strips and the skin plates are presented. Results of field pulling tests on the reinforcement are also included.

EMBANKMENT GEOMETRY

The reinforced earth fill is constructed on top of a random fill embankment founded over the slide debris. At the bottom of the slide debris a toe buttress was built to act as a

ClibPDF - www.fastio.com

stabilizing fill embankment. The overall height of the system is approximately 360 feet. The reinforced earth fill has a maximum height of 55 feet and a length of 528 feet. A system of surface and subsurface drain pipes were installed to remove surface water and seepage. The embankment is shown in plan and profile by Figure 1.

DESIGN OF REINFORCEMENT

Referring to Figures 2 and 3 and based on Rankine's state-of-stress theory, the two basic equations for designing the reinforcement developed by Chang, et al (2) are as follows:

Tensile Stresses

$$f_s = \frac{K_a \gamma H d \Delta h}{bt} \tag{1}$$

Factor of Safety Against Slippage

$$F.S. = \frac{2F}{T} = \frac{b L \tan \delta}{6K_a d \Delta h} \quad \text{(English Unit)} \tag{2}$$

$$= \frac{b L \tan \delta}{50 K_a d \Delta h} \quad \text{(SI Units)}$$

Where:

f_s = steel tensile stress in psi (kilograms per square centimeter)

K_a = Rankine active earth pressure coefficient

b = steel strip width in inches (centimeters)

t = steel strip thickness in inches (centimeters)

γ = soil density in pounds per cubic foot (kilograms per cubic meter)

ClibPDF - www.fastio.com

H = overburden height in feet (meters)

d = steel strip horizontal spacing in feet (meters)

Δh = steel strip vertical spacing in feet (meters)

T = tensile force in steel strip in pounds (kilograms)

F = frictional resistance in pounds (kilograms)

L = length of steel strip in feet (meters)

δ = friction angle between steel and soil in degrees

These equations were used to compute the theoretical steel stresses for comparison with those measured by field instrumentation.

DESIGN OF SKIN PLATES

The standard shape of the skin plate, used by the French firm, Terre Armee, consists of a semi-elliptical element of 10 to 13 inches (25 to 33 centimeters) high with a thickness of about 1/8 inch (3 mm).

For the purpose of simplifying the stress analysis, the following were assumed: (1) semicircular section of skin plate; (2) soil pressure distribution and deformation configuration shown by Figure 4; (3) a vertical load, P, representing a resultant force transferred from a uniform vertical pressure acting along an effective length of reinforcing strip will cause a vertical deformation, δ_v. This vertical deformation is assumed to have the same magnitude as the settlement of the soil mass caused by a uniform vertical soil pressure acting on the top and bottom row of reinforcement.

ClibPDF - www.fastio.com

Using strain energy principles described by Sealy and Smith (3), the equations for computing the vertical load, P, and the end moment, M_a, were developed as follows:

For hinged end conditions (Figure 4),

$$P = \frac{4EI\delta_v}{R^3\pi} - \frac{4K_a\gamma HR}{3\pi} - \frac{\gamma HR}{24\pi}(3\pi - 32)\,; \tag{3}$$

and for fixed end conditions (Figure 4),

$$P = \frac{\delta_v EI}{\pi R^3}\left(4 - \frac{32}{8-\pi^2}\right) + \gamma HR\left(\frac{4-4K_a}{3\pi} - \frac{1}{8}\right) - \frac{8\gamma HR}{8-\pi^2}\left(\frac{4-4K_a}{3\pi} - \frac{(1+\pi-\pi K_a)}{8} + \frac{1}{9}\right); \tag{4}$$

and

$$M_a = \frac{8\delta_v EI}{R^2(8-\pi^2)} + \frac{2\pi\gamma HR^2}{(8-\pi^2)}\left(\frac{4-4K_a}{3\pi} - \frac{(1+\pi-\pi K_a)}{8} + \frac{1}{9}\right). \tag{5}$$

The magnitude of P depends upon the restraint conditions at the ends and the value of vertical settlement, δ_v. Once the unknown load, P, and the unknown bending moment, M_a, (Figure 4) are determined, the stresses developed in the skin plate can be calculated. Equations 3, 4 and 5 can be solved by measuring the vertical deformations, δ_v, in field performance studies or laboratory scale model tests. For design purposes, a value of δ_v, can be determined by estimating the embankment settlement.

ClibPDF - www.fastio.com

CONSTRUCTION MATERIAL

Triaxial tests (consolidated drained condition) on the backfill material resulted in a friction angle, ϕ, of 40 degrees at 95% relative compaction. From this, Rankine's coefficient of active earth pressure, K_a, was calculated to be 0.22. The coefficient of earth pressure at rest, K_o, was found to be 0.36 based on J. Jaky's (4) expression, $K_o = 1-\sin\phi$. Laboratory skin friction tests between the galvanized steel strip and the soil were conducted using a specially designed shear box resulted in a skin friction angle of 31°.

The dimensions of the steel reinforcing strips provided by Terre Armee were as follows:

Thickness	0.118 inches (3 mm)
Width:	2.362 inches (60 mm)
Length:	22.79 feet to 46.0 ft. (7 meters to 14 meters)

Laboratory tests resulted in a yield strength of 37,000 psi, (108,300 Kg/cm^2), ultimate strength of 50,000 psi (146,300 Kg/cm^2), Young's modulus of 28.5 x 10^6 psi (88.390 x 10^6 Kg/cm^2) and a Poisson's ratio of 0.28.

INSTRUMENTATION

In order to monitor the behavior of the completed structure, comprehensive instrumentation was installed in the field. Included were (1) slope indicators to measure internal movement of the embankment and slide debris; (2) settlement platforms to

ClibPDF - www.fastio.com

measure vertical settlements; (3) extensometers to measure soil strains; (4) soil pressure cells to measure soil stresses; (5) strain gages to measure stresses developed in the reinforcing strips and skin plates; and (6) gage points to measure deformations of the skin plates and the wall face. Locations of the instruments are shown in Figures 1 and 5.

All instruments were read periodically during construction and for approximately one year after completion of the embankment.

STRESSES IN THE REINFORCING STRIPS

The daily history of the axial stresses in the steel strips is shown in Figure 6. They were calculated based upon average strain recorded on top and bottom of the strip and the modulus of elasticity of 28.5×10^6 psi (83.391×10^6 Kg/cm^2).

For comparison, the steel stresses assuming the active earth pressure and "at rest" cases were computed using equation 1 and superimposed on Figure 6.

At Station 550+25, the lowest axial stresses were measured near the wall face. After completion of the fill, the stresses near the wall face decreased with time and eventually became compressive at level A. This phenomenon was probably due to the restraint provided by the berm. At 15 and 25 feet from the wall face, the stresses in the strips increased with time finally reaching the calculated stress, σ_a, based on coefficient of active pressure, K_a. At Level B, the steel stresses at 15

ClibPDF - www.fastio.com

feet from the wall face decreased with time to values much lower than σ_a, while the stresses at 25 feet from the wall face increased with time approaching the calculated stress, σ_o, based on coefficient of earth pressure at rest, K_o. At Level C, the magnitude of all steel stresses decreased with time, approaching σ_a.

At Station 551+75, all strips on Level A were in compression with the maximum stresses developed very near the wall face. This phenomenon was probably due to the restraint provided by the berm, since Level A is about 10 feet below the top of the berm. At Level B, all strips were stressed in tension with the magnitude much less than σ_a near the wall face and at 30 feet from the wall face. The strip stress at 15 feet from the wall face approached σ_a, however. At Level C, all steel stresses increased with time. The last reading indicated a stress approaching σ_a near the wall face and exceed σ_a at 15 and 30 feet.

SOIL STRESSES

Figure 7 presents the soil stresses measured at Station 551+75. The ratio, K, between the horizontal stress and vertical stress is also plotted on this figure. The γH lines represent the theoretical vertical soil stresses computed using a unit weight, γ, of 143 pounds per cubic foot (2290 Kgs per cubic meter) and the corresponding depth of fill, H, over each instrumentation level. The K values varied irregularly during

ClibPDF - www.fastio.com

and immediately after construction presumably due to the effect of the compaction operation. As the height of fill increased over the instrumentation level, the influence of compaction diminish. After completion of the fill, the K values still varied between 0.11 and 0.41 as compared to the calculated K_a of 0.22 and K_o of 0.36.

STRESSES IN THE SKIN ELEMENTS

Figure 8 shows the daily history of stresses in the skin element. The locations and the identification numbers of the strain gages are shown on top of the figure. Gages 1, 5 and 9 measured axial strains on the outside of the face while Gages 3, 7 and 11 measured axial strains on the inside. Gages 2, 6 and 10 measured circumferential strain on the outside of the face, while Gages 4, 8 and 12, the circumferential strain on the inside. The actual deformation of the skin elements closely approximated the deformation assumed in developing equations 3, 4 and 5. Accordingly, tensile circumferential stresses developed on the outside of the face, and compressive circumferential stresses on the inside.

Deformations of the skin elements were measured at 5 gage points on the faces of the skin plates with a specially designed vernier-micrometer caliper capable of accurately measuring to one thousandth of an inch.

The measured relationship between the vertical deformation of the skin plate and fill height is shown in Figure 9. Based

ClibPDF - www.fastio.com

on the vertical deformations observed in the field, the stresses in the skin plates were calculated, for both hinged and fixed end conditions. A comparison of the measured and computed circumferential stresses is also shown in Figure 9. The calculated stresses based on hinged end assumption (Equation 3) agree reasonably well with the measured data, while the calculated stresses based on the fixed end condition (Equations 4 and 5) are almost three times larger than those measured.

FIELD PULLING TESTS

In order to test the validity of Equation 2, dummy reinforcing strips were installed in the fill at 5 levels for field pulling tests. Three strips, 5, 10, and 15 feet in length, were embedded at each of three levels under overburden heights of 7.5, 12.4, and 18.2 feet. Three 23-foot strips were embedded at a depth of 18 feet, as were three 46-foot strips at a depth of 38 feet. One, each, of the 23-foot and 46-foot strips was instrumented with strain gages on both top and bottom at 5-foot intervals.

A typical load deformation curve obtained from field pulling tests are shown in Figure 10-a for a 5-foot strip. Three pulling loads were defined for analysis and indicated on the curves. These were (1) yield loads representing the proportional limit of the load-deformation relationship; (2) peak load representing the maximum pulling load; and, (3) the residual load representing the pulling load when deformation increased

ClibPDF - www.fastio.com

appreciably without change in the pulling load.

Figure 10-b presents the relationships between the pulling loads, the overburden height, and strip length. The skin-friction angles, ϕ_u, of 31 degrees obtained from the residual pulling load plots agree well with the laboratory test results at equal overburden pressure.

It is interesting to note that under a constant overburden height, the residual loads are proportional to the overburden loads which are the products of the overburden height, H, the unit weight, γ, the width of steel strip, b, and the length of the steel strip, L. Since γ, b, and H are constant under a given overburden height, the residual loads are proportional to the strip length. Because the peak load represents the maximum mobilized friction grip, it was utilized to calculate the factor of safety for the failure condition. The design tensile loads were calculated using Equation 1. The relationships between overburden height, H, strip length, L, and factor of safety are shown in Figure 10-c, for a fill height of 10 feet, the minimum strip length may require only 9 feet for a factor of safety of 4.

AXIAL FORCES IN DUMMY STRIPS DUE TO STATIC LOADING

Figure 10-d, shows the relationship between overburden loads and the maximum axial force observed in the 46-foot and the 23-foot strips at 10 to 15 feet from the wall face. The axial forces developed during construction are all lower than the calculated

ClibPDF - www.fastio.com

tensile force, T_a, from Equation 1, based on the Rankine's active earth pressure coefficient, K_a. However, after the fill was completed the axial force continued to increase and the maximum axial force reached T_a, in the 23-foot strip. In the 46-foot strip, the maximum axial force finally reached T_o, the calculated tensile force from Equation 1, based on the "at rest" earth pressure coefficient, K_o. The continuous increase in tensile force after completion of the fill was probably due to the continuing settlement. During the time at completion of construction and 8 months thereafter, the settlements on Level B and C, Station 551+75, varied from 1.5 to 2.5 feet (0.46 to 0.76 meters). However, on Level A, the settlement varied from 2.5 to 3.5 feet (0.76 to 1.07 meters). It has been also observed that the face of the wall has moved a maximum of 0.7 feet (0.21 meters) horizontally downslope since completion of the fill. Both horizontal movement and settlement are attributed primarily to densification of the uncompacted slide debris.

SUMMARY AND CONCLUSIONS

1. The measured vertical soil stresses generally agree with the calculated vertical earth pressures. The stress ratios, K, between the horizontal and vertical soil stresses were highest during the early stages of construction and then decreased after completion of the fill with large variations from point to point.

ClibPDF - www.fastio.com

2. The measured stresses in the steel strips near the wall face were generally smaller than, but approached the calculated theoretical stresses, σ_a, based on Rankine's active stress condition. The highest steel stresses developed in the inner middle portion of the reinforced earth section. The steel stresses may increase to the values corresponding to theoretical "at rest" earth pressure.

   Equation 1 presented in this paper for the design of reinforcing strips has been verified. The use of the active earth pressure coefficient, K_a, for calculating the steel stress is applicable for the end portion of the reinforcements. For the middle portion of the reinforcement, the K_o (the coefficient of earth pressure "at rest") should be used in design.

3. Field pulling test results indicate that the load-deformation curves resembled the stress-strain curves obtained from laboratory triaxial compression tests on dense sand, when the strips were pulled loose. The yielding, peak, and residual load points are all defined clearly. The frictional forces developed on the steel strips were proportional to the overburden load for each overburden height. The field measured skin friction angle agreed well with the laboratory test results under equal overburden height.

ClibPDF - www.fastio.com

The relationships between the overburden height, strip length, and the factor of safety against slippage shown in Figure 10-c can be used for determining the minimum length of reinforcement, providing the requirement for stability is met.

4. The structural behavior of the skin plates followed the hinged end assumption in deformed shape and stress values. The vertical deformation of the skin plate, which is a measurement of settlement within each skin element, is proportional to the overburden height.

   Design Equation 3, developed in this paper for design of the steel skin plate, accurately predicted the stresses developed in the skin plate. Use of the vertical deformation, δ_v, of the skin plate for one of the major functions in design has proven to be a satisfactory approach.

   Figure 9-b can be used for estimating the vertical deformation, δ_v, for design of skin plate at different height of reinforced earth fill. The assumption of a semi-circular shape simplified the calculation of the stresses in the skin plate and accurately predicted the measured stresses.

ClibPDF - www.fastio.com

5. The settlement and horizontal movement of the reinforced earth embankment is primarily attributable to the densification of the deep foundation slide debris. These movements are probably the main cause of continuing change in stresses of the steel and soil after completion of the fill.

ClibPDF - www.fastio.com

ACKNOWLEDGEMENT

This paper presents the results of a Federally-financed research project. The writers wish to acknowledge and thank Gary Bork and John Kenan who were in charge of overall project design for their valuable assistance. The patience and cooperation of Robert F. Britton, the Resident Engineer, who provided valuable assistance in installing the instrumentation during construction is also gratefully acknowledged.

This work was done under the HPR Work Program in cooperation with the U.S. Department of Transportation, Federal Highway Administration.

The contents of this paper reflect the views of the authors, who are responsible for the facts and the accuracy of the data presented herein. The contents do not necessarily reflect the official views or policies of the State of California or the Federal Highway Administration. This paper does not constitute a standard, specification, or regulation.

ClibPDF - www.fastio.com

REFERENCES

1. Vidal, Henri, "The Principle of Reinforced Earth," Highway Research Record, Number 282, pp 1-16, Washington, D.C., 1969.

2. Chang, Jerry C., Forsyth, Raymond A., and Smith, Travis W., "Reinforced Earth Highway Embankment - Road 39," Highway Focus, Volume 4, Number 1, January 1972, Federal Highway Administration, U.S. Department of Transportation.

3. Seely, F. B. and Smith, J. O., Advanced Mechanics of Materials, John Wiley and Sons, Inc., New York, July 1962, pp 421-437.

4. Jaky, J., "Pressure in Silos," Proc. 1st Conf. on Soil Mechanics and Foundation Engineering (Rotterdam) 1948.

ClibPDF - www.fastio.com

ClibPDF - www.fastio.com

ClibPDF - www.fastio.com

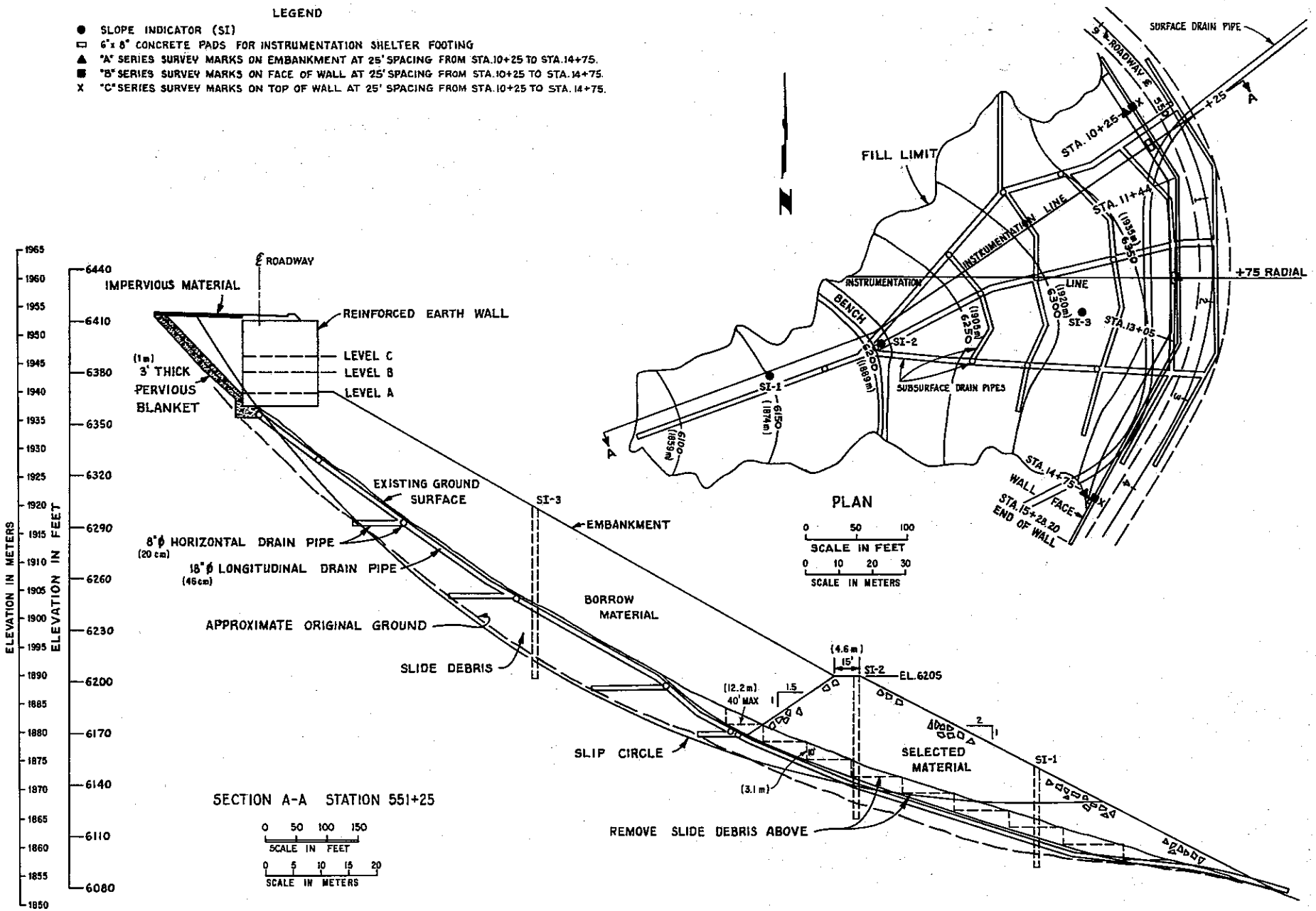

PLAN AND PROFILE

FIGURE 1

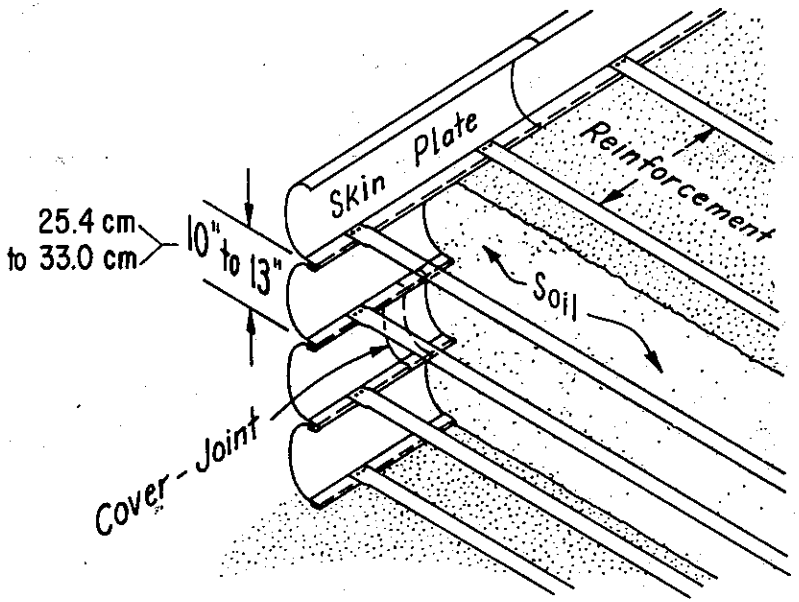

Figure 2 SCHEMATIC OF REINFORCED EARTH FILL

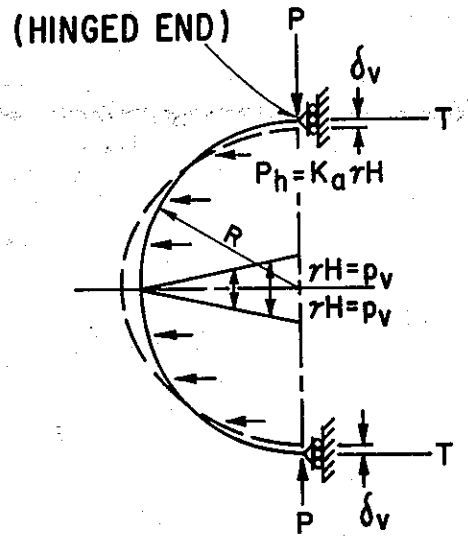

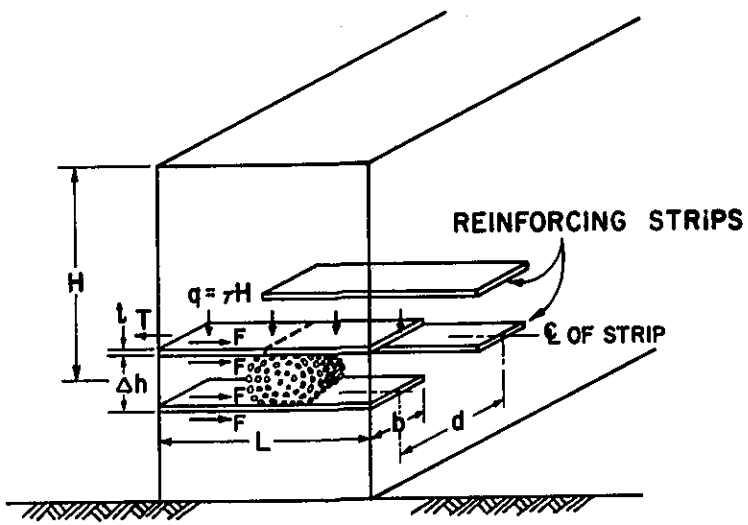

Figure 3

SCHEMATIC OF REINFORCED EARTH BLOCK

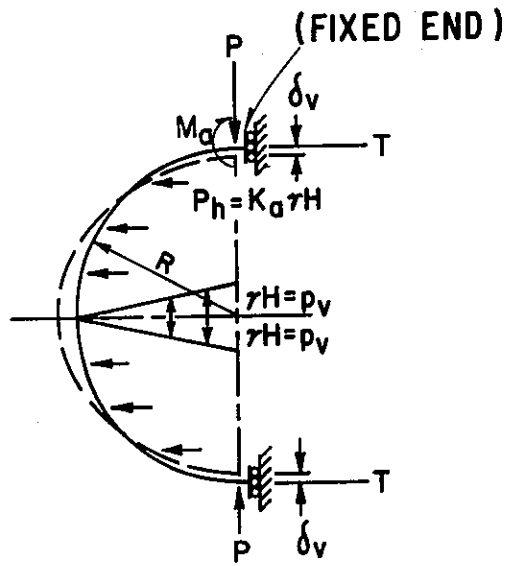

Figure 4

LOADING DIAGRAM ON SKIN PLATE

ClibPDF - www.fastio.com

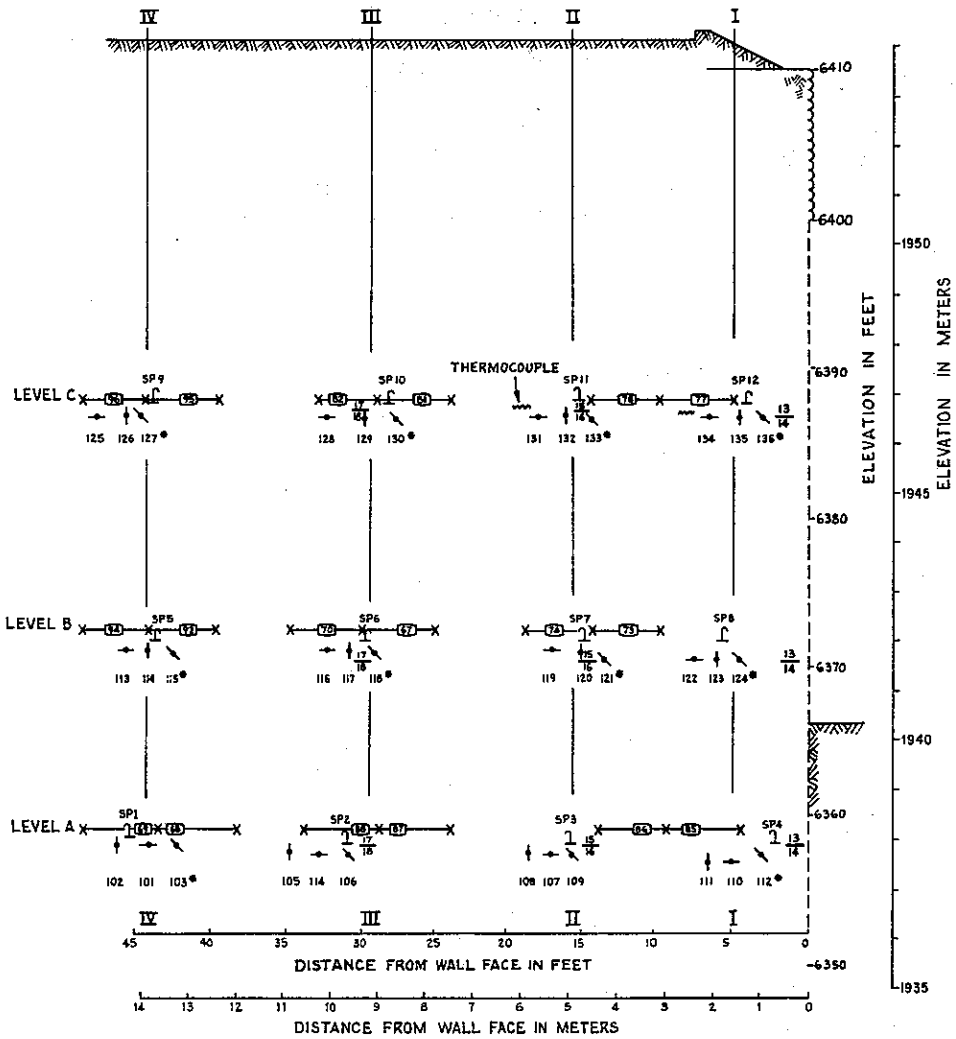

INSTRUMENTION SECTION
STA 551+75

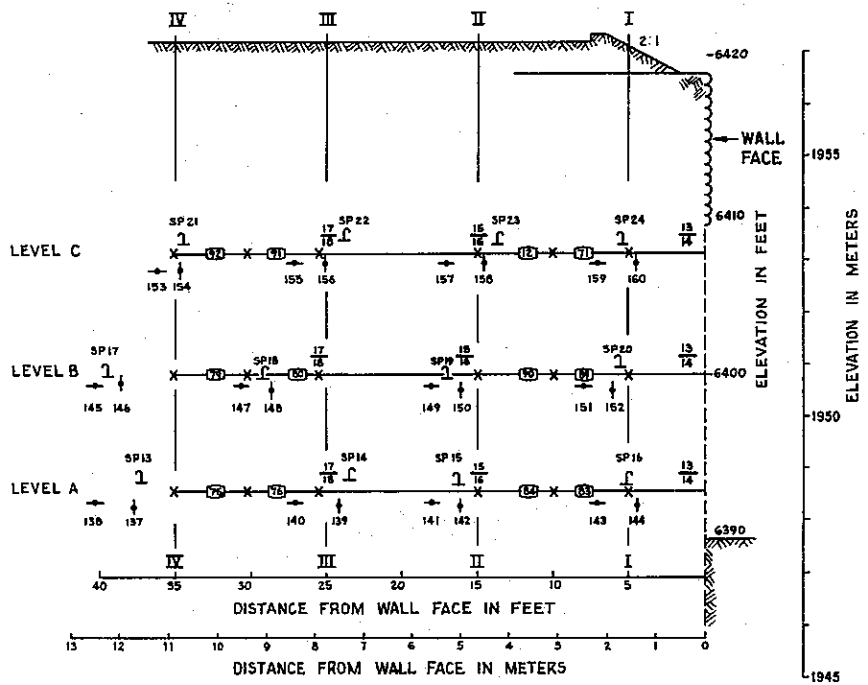

INSTRUMENTION SECTION
STA 550+25

LEGEND

SP9 SETTLEMENT PLATFORM

55 EXTENSOMETER

17/18 STRAIN GAGE ON STRIP

116 117 118* PRESSURE CELLS WITH CORRESPONDING INDENTIFICATION NUMBER BENEATH THE CELL. CELL I.D. NUMBERS WITH ASTORISK (*) INDICATES A GENTRAN PRESSURE CELL. ALL OTHERS ARE GLOETZL PRESSURE CELLS.

INSTRUMENTATION SECTIONS

FIGURE 5

ClibPDF - www.fastio.com

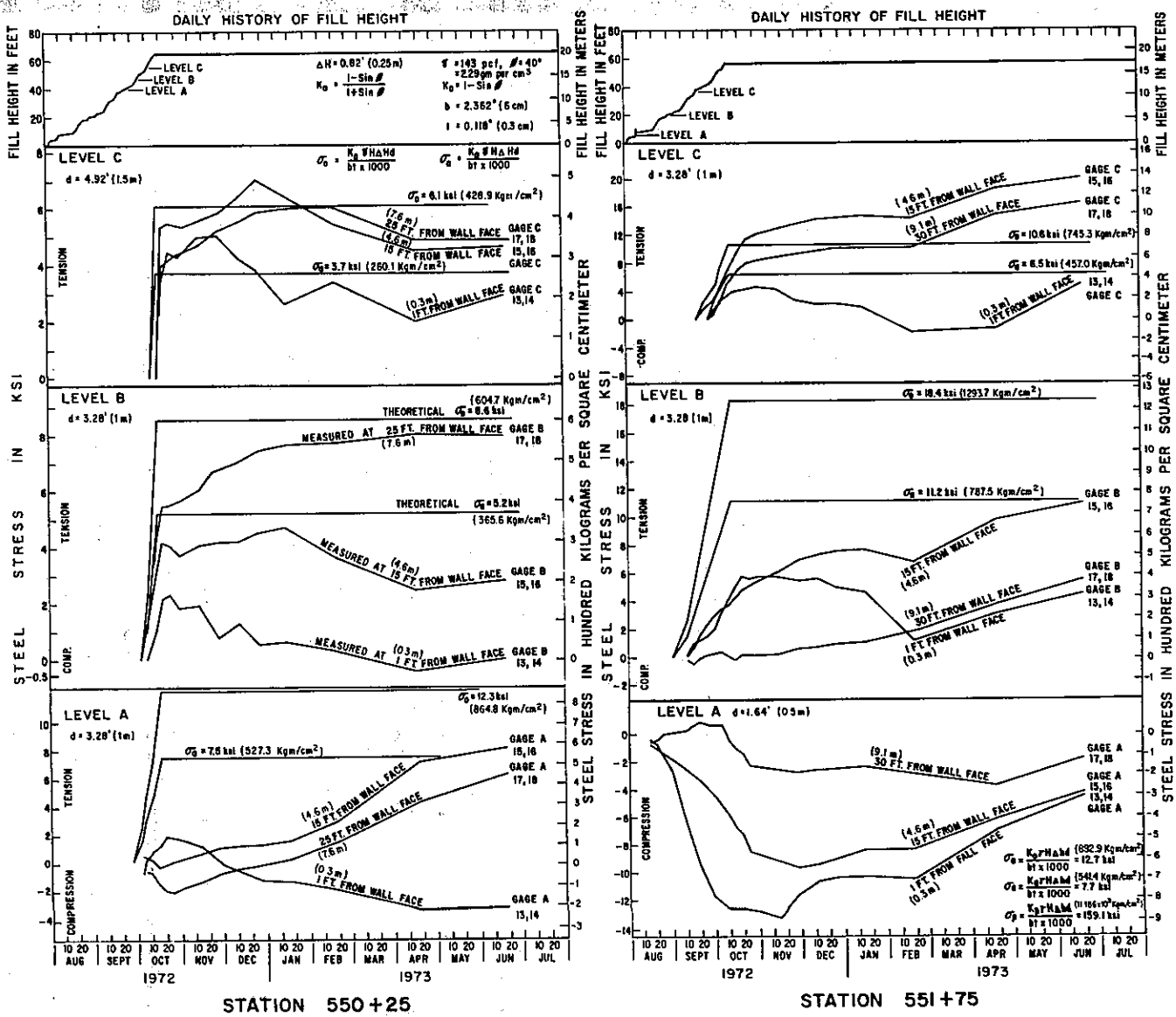

DAILY HISTORY OF STRESSES IN STEEL STRIP

FIGURE 6

ClibPDF - www.fastio.com

DAILY HISTORY OF FILL HEIGHT

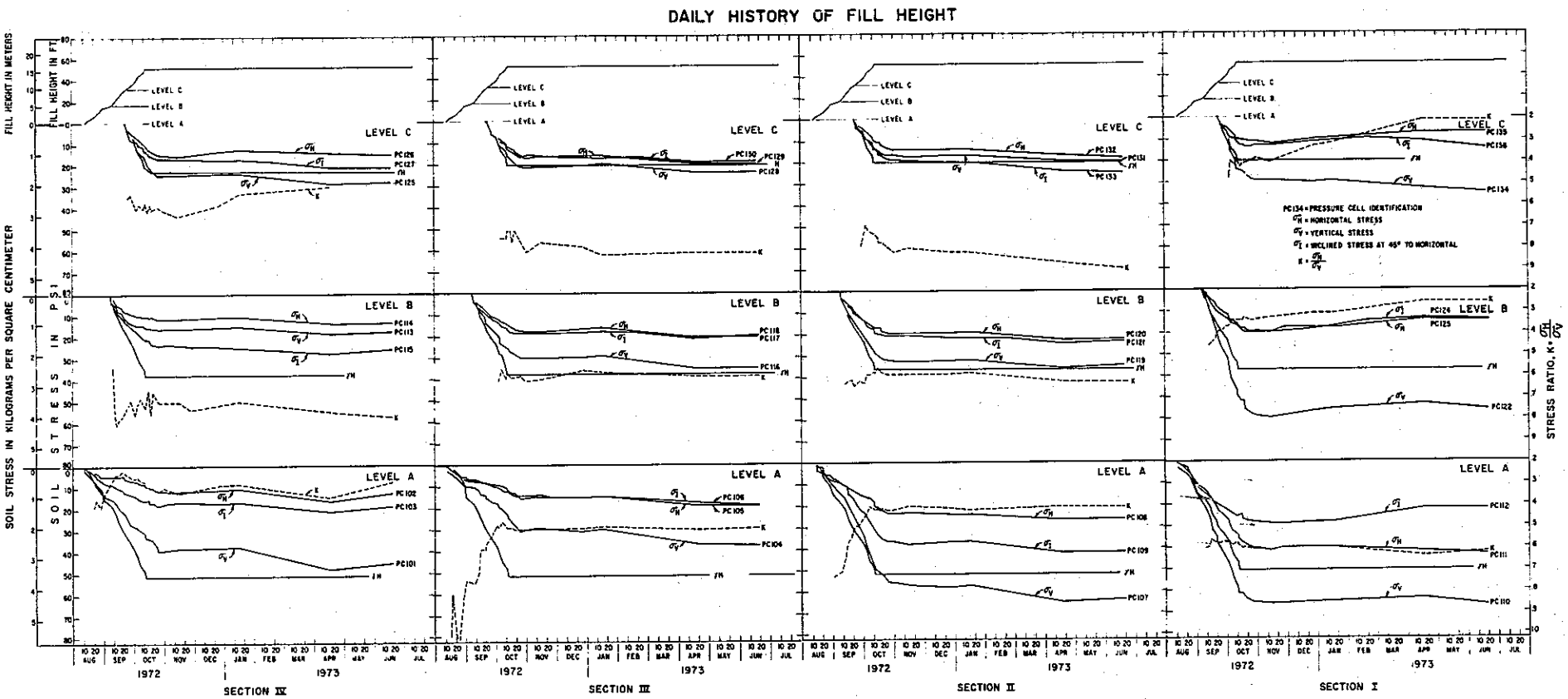

STATION 551+75

DAILY HISTORY OF SOIL STRESS

FIGURE 7

ClibPDF - www.fastio.com

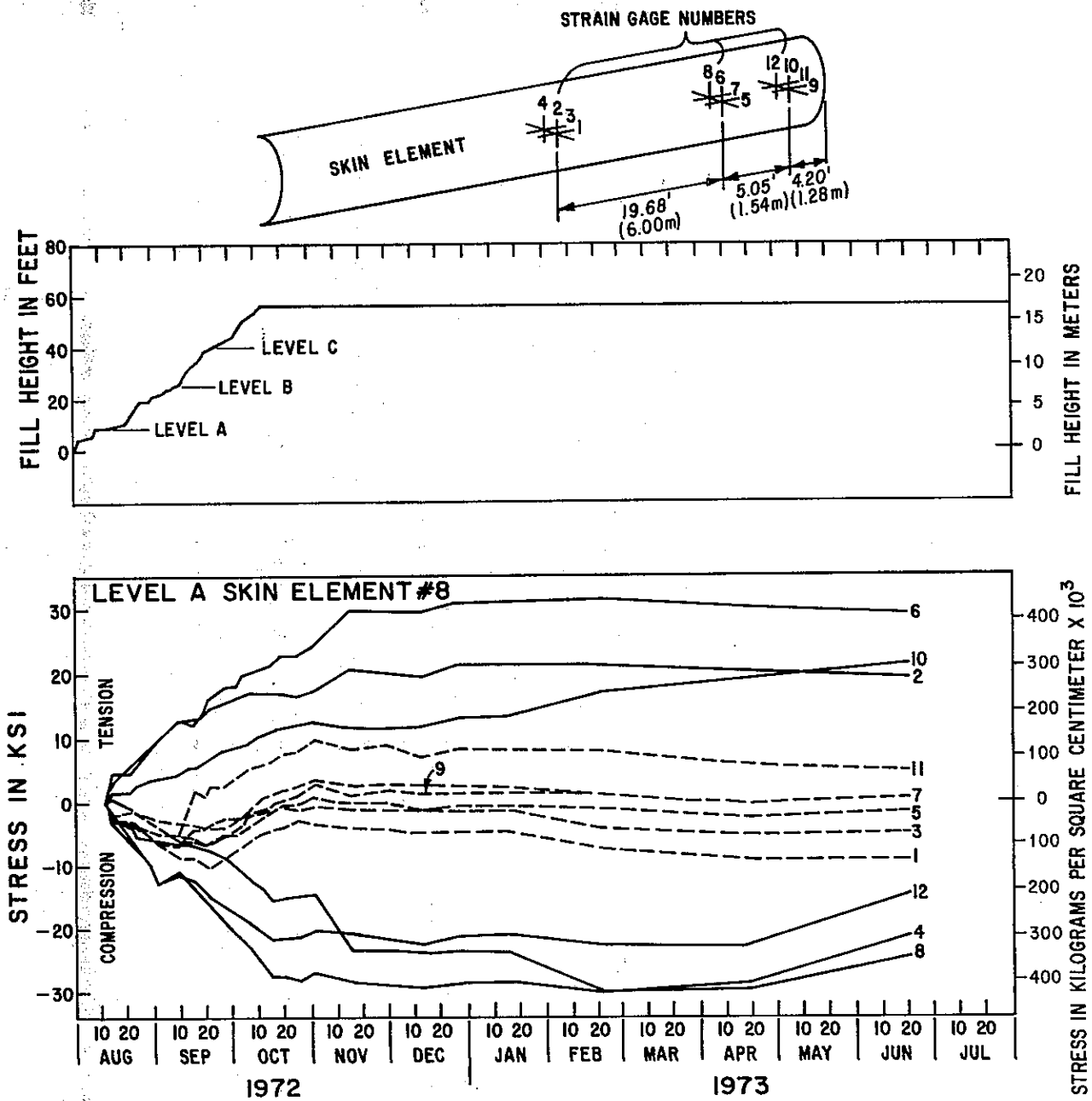

STATION 551+75

DAILY HISTORY OF STRESS IN SKIN ELEMENT

GAGE NOS.	POSITION
6, 10, 2	OUTSIDE CIRCUMFERENTIAL
4, 8, 12	INSIDE CIRCUMFERENTIAL
1, 5, 9	OUTSIDE TARGENTIAL
3, 7, 11	INSIDE TARGENTIAL

FIGURE 8

ClibPDF - www.fastio.com

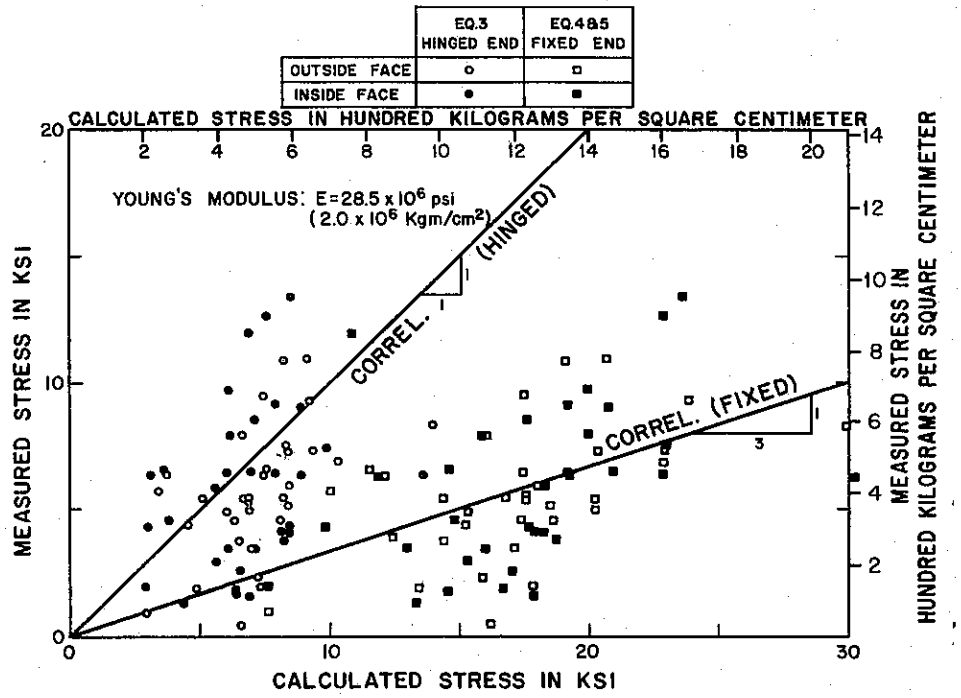

(a) COMPARISON OF MEASURED AND CALCULATED CIRCUMFERENTIAL STRESS AT SPRING LINE OF SKIN PLATE

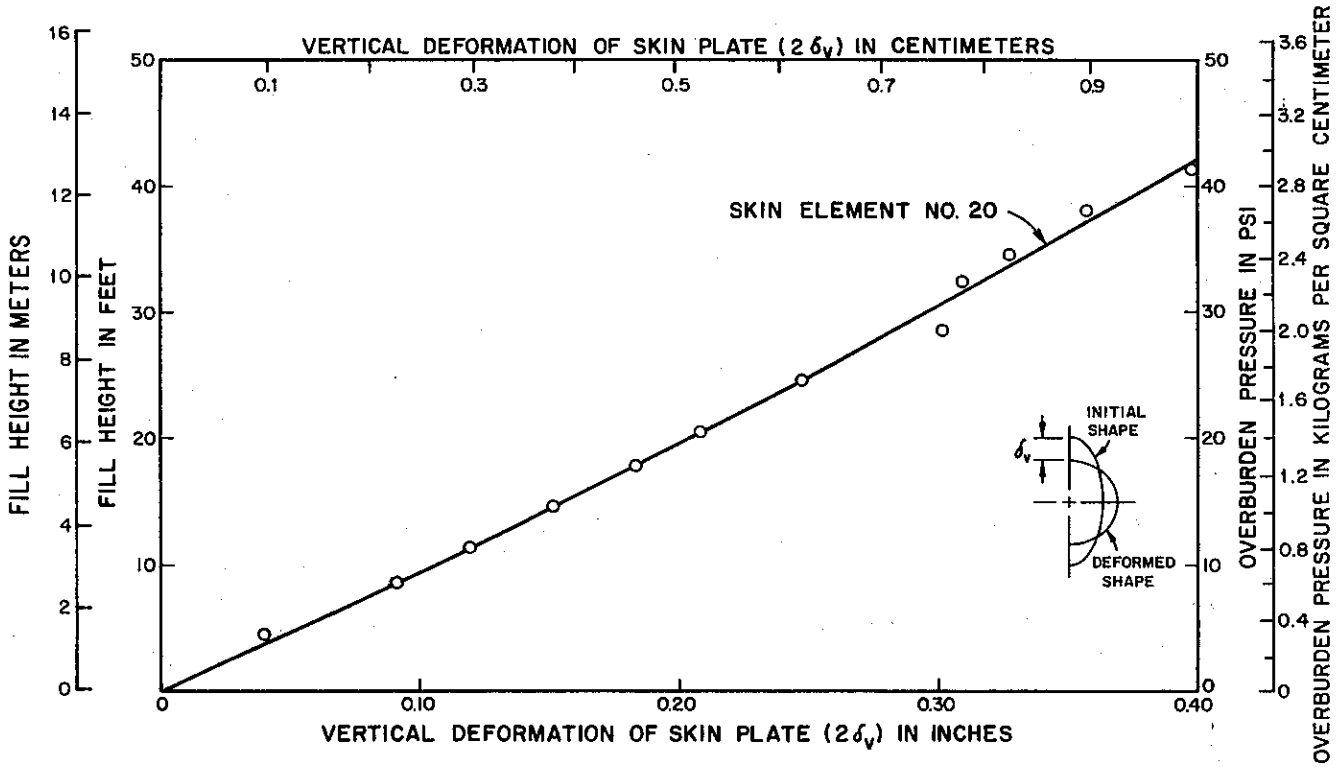

(b) RELATIONSHIP BETWEEN FILL HEIGHT AND SKIN PLATE DEFORMATION STATION 551+75

FIELD BEHAVIOR OF STEEL SKIN ELEMENT
FIGURE 9

ClibPDF - www.fastio.com

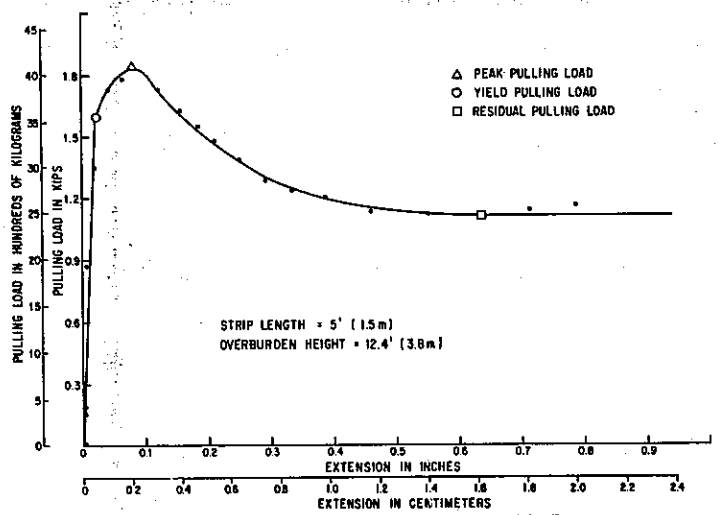

(a) TYPICAL LOAD DEFORMATION CURVE

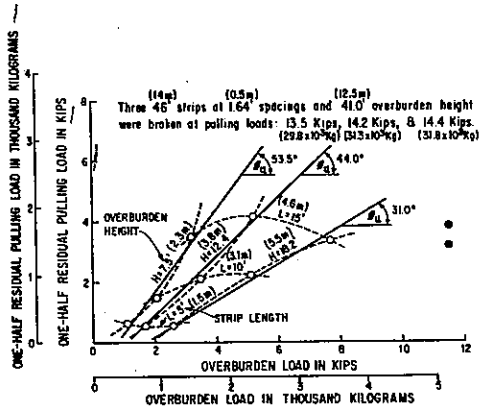

(b) RELATIONSHIP BETWEEN RESIDUAL PULLING LOAD, OVERBURDEN LOAD, OVERBURDEN HEIGHT AND STRIP LENGTH

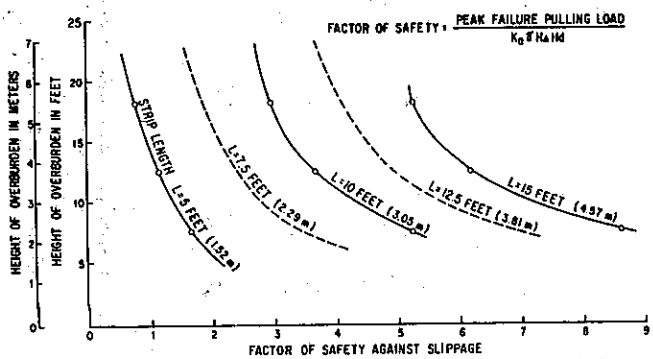

(c) RELATIONSHIP BETWEEN OVERBURDEN HEIGHT, STRIP LENGTH, AND SLIPPING FACTOR OF SAFETY

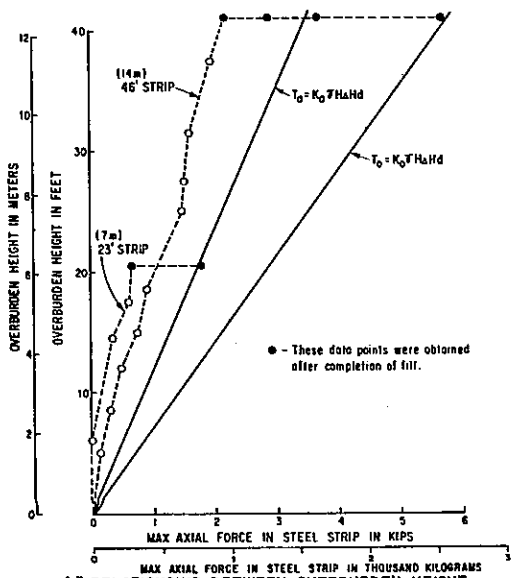

(d) RELATIONSHIP BETWEEN OVERBURDEN HEIGHT AND AXIAL FORCE IN STEEL STRIP

FIELD PULLING TEST RESULTS

FIGURE 10

ClibPDF - www.fastio.com

ClibPDF - www.fastio.com

ClibPDF - www.fastio.com